

Lattice dynamics in the charge-density-wave metal at a van-Hove-singularity filling

Jia-Wei Mei,^{1,2,*} Fei Ye,^{1,2,†} and Xiaobin Chen^{3,‡}

¹Shenzhen Institute for Quantum Science and Engineering, and Department of Physics, Southern University of Science and Technology, Shenzhen 518055, China

²Shenzhen Key Laboratory of Advanced Quantum Functional Materials and Devices, Southern University of Science and Technology, Shenzhen 518055, China

³School of Science and State Key Laboratory on Tunable Laser Technology and Ministry of Industry and Information Technology Key Lab of Micro-Nano Optoelectronic Information System, Harbin Institute of Technology, Shenzhen 518055, China

(Dated: April 12, 2022)

The charge-density-wave (CDW) order with macroscopically occupied electrons distorts the underlying lattice and usually causes the softening of the associated phonon mode. However, previous studies demonstrated that the spin-Peierls transition does not always induce an associated phonon softening, but the central-peak scenario applied in the quasi-one-dimensional compound CuGeO₃. We generalize the lattice-dynamics studies on the two-dimensional CDW state at van-Hove-singularity (VHS) filling and find that the CDW ordering could develop a central peak at zero frequency while the associated phonon undergoes hardening. The particle-hole scatterings between VHS points give rise to a low-energy increased charge-density susceptibility, and their coupling to the lattice dynamics induces two poles in the Green function for the CDW-associated phonon mode. The zero-frequency pole corresponds to the collective charge-density and phonon coupling mode. The high-frequency one is related to the high-temperature phonon mode that hardens as reaching the CDW transition. Our result may have the potential implication for the recently discovered Kagome metal AV₃Sb₅ ($A = \text{K, Rb, Cs}$) in which no soft phonon is observed during the CDW transition.

Introduction.— The low-energy excitation in metal gives rise to an increased bare electron charge-density susceptibility $\chi_0(\mathbf{Q})$ with the wave vector \mathbf{Q} connecting two extreme points at the Fermi surface. Thus a periodic potential, e.g. through the electron-phonon interaction, will cause an electronic charge-density modulation as $\Delta\rho(\mathbf{Q}) = \chi^0(\mathbf{Q})V(\mathbf{Q})$. As feedback, the charge-density fluctuation modifies the periodic potential. It renormalizes the phonon frequency, $\omega^2(\mathbf{Q}) = \Omega_0^2(1 + \kappa\chi_0(\mathbf{Q}))$, where Ω_0 is the bare phonon spectrum, leading to the softening of $\omega(\mathbf{Q})$, known as the Kohn anomaly [1]. When it reduces the phonon frequency to zero, the charge-density modulation induces a static lattice distortion, leading to the charge-density-wave (CDW) order [2, 3]. Rare-earth tritellurides RTe₃ are prime examples of CDW ordered ground states where the phonon softening appears near the CDW transition temperature T_{CDW} [4–6]. Unexpectedly, in the recent kagome compounds AV₃Sb₅ ($A = \text{K, Rb, Cs}$), which exhibit intertwined CDW order and superconductivity [7–10], no CDW-associated phonon softening is observed in the X-ray and neutron scatterings [11, 12]. Even more puzzling, the neutron scattering reveals the phonon hardening during the CDW transition in CsV₃Sb₅ [12]. The origin of the CDW in AV₃Sb₅ probably mainly arises from collective particle-hole scattering between the van-Hove-singularity (VHS) M -points [13–16], which enhances the charge-density fluctuations and modifies the lattice dynamics.

The puzzled phonon behaviors in AV₃Sb₅ motivate us to study the lattice dynamics in the CDW metal at the kagome VHS filling in this paper. To simplify the problem, we study

a phenomenological model that describes the coupling of a single CDW-associated phonon mode and the charge-density fluctuations near the Fermi surface on the random-phase-approximation (RPA) level. Such a model belongs to the Fano problem for a discrete phonon mode embedding in the charge-density-fluctuation continuum. We tune the electron-electron interaction u and electron-phonon coupling κ to induce the CDW transition within RPA phenomenologically. Within proper parameters in the CDW metal at VSH filling, a central peak appears in the phonon dynamic structural factor as we approach the CDW transition. Meanwhile, the CDW-associated phonon frequency becomes hardening, instead of softening. The related central-peak physics has previously been discussed similarly in the famous spin-Peierls insulating compound CuGeO₃ [17–19], in which the phonon frequency is much larger than the spin-Peierls transition temperature. For a comparative study, the soft phonon mode is found in the lattice dynamics in the CDW order induced by the nesting of nearly parallel quasi-1D Fermi surface, consistent with experiments in the CDW compound RTe₃. By analysis of the pole structure, the phonon Green function has one pole for the soft-phonon scenario while it has two poles in the central-peak regime in which the zero-frequency pole corresponds to the collective charge-density and phonon coupling mode and the high-frequency one is related to the high-temperature phonon mode. Our simple RPA theory may have the potential implication for the absence of the soft-phonon mode in AV₃Sb₃ although its more complicated multiple-band structure crossing the Fermi level requires further investigations.

RPA methods and related experimental parameters. — Given the band dispersion $\epsilon_{\mathbf{k}}$, the density of states (DOS) at Fermi level with $\omega = 0$ is approximated as

$$\text{DOS}(\mathbf{k}) = -\frac{2}{\pi} \text{Im} \int_{-\Delta\omega}^{\Delta\omega} \frac{d\omega'}{\omega' + i\delta - \epsilon_{\mathbf{k}}}, \quad (1)$$

* meijw@sustech.edu.cn

† yef@sustech.edu.cn

‡ chenxiaobin@hit.edu.cn

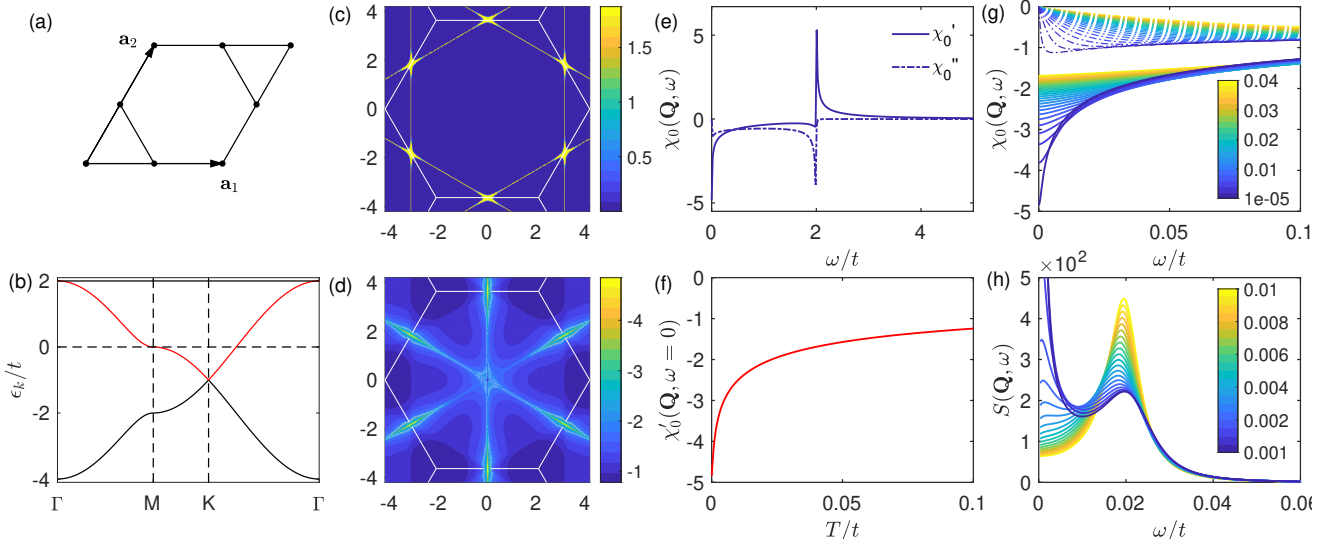


FIG. 1. Central peak for kagome VHS filling. (a) Kagome lattice with primitive unit vectors $a_1 = (1, 0)$ and $a_2 = (1/2, \sqrt{3}/2)$. (b) Band dispersion of the simple kagome model along the high-symmetry direction. (c) \mathbf{k} -dependent DOS(\mathbf{k}) as in Eq. (1) where the VHS points at M displays the enhanced value. (d) \mathbf{q} -dependent static charge-density susceptibility $\chi_0(\mathbf{q})$ at low temperature $T = 0.00001t$ with an enhanced amplitude at the CDW wave vectors \mathbf{Q} with $(k_1, k_2) = (0, \pi), (\pi, 0), (\pi, \pi)$. (e) ω -dependent $\chi(\mathbf{Q}, \omega)$ at low temperature $T = 0.00001t$. The solid and dotted lines are the real and imaginary parts, respectively. (f) Temperature-dependent static charge-density susceptibility $\chi(\mathbf{Q}, \omega = 0)$. (g) Temperature evolution of ω -dependent $\chi(\mathbf{Q}, \omega)$. The solid and dotted lines are the real and imaginary parts, respectively. (h) Temperature evolution of the dynamical structure factor $S(\mathbf{Q}, \omega)$ with $u/\kappa = 0$ for $T_{\text{CDW}} = 0.001t$. The color bars in (g) and (h) represent the temperature value in the unit of t .

and the charge density $\rho(\mathbf{q}) = \sum_{\mathbf{k}\sigma} c_{\mathbf{k}+\mathbf{q}\sigma}^\dagger c_{\mathbf{k}\sigma}$ has the susceptibility

$$\chi(\mathbf{q}, i\omega_n) = \frac{1}{V} \int_0^\beta e^{i\omega_n \tau} \rho(\mathbf{q}, \tau) \rho(-\mathbf{q}, 0) d\tau, \quad (2)$$

which represents the particle-hole bubble diagram for non-interacting electrons

$$\chi_0(\mathbf{q}, i\omega_n) = 2 \int \frac{d^2k}{(2\pi)^2} \frac{n_F(\epsilon_{\mathbf{k}}) - n_F(\epsilon_{\mathbf{k}+\mathbf{q}})}{i\omega_n + \epsilon_{\mathbf{k}} - \epsilon_{\mathbf{k}+\mathbf{q}}}. \quad (3)$$

On the RPA level, the electron-electron interaction renormalizes the susceptibility

$$\chi(\mathbf{q}, i\omega_n) = \frac{\chi_0(\mathbf{q}, i\omega_n)}{1 - u\chi_0(\mathbf{q}, i\omega_n)}. \quad (4)$$

The effective interaction, e.g. the off-site interactions [20], causes the CDW transition at the CDW wave vector \mathbf{Q} if

$$1 - u\chi_0(\mathbf{Q}, 0) = 0. \quad (5)$$

The collective charge-density mode leads to the RPA phonon Green function

$$D(\mathbf{Q}, i\omega_n) = \frac{2\Omega_0}{(i\omega_n)^2 - \Omega_0^2(1 + \kappa\chi(\mathbf{Q}, i\omega_n))}, \quad (6)$$

where Ω_0 is the bare frequency and κ denotes the electron-phonon coupling strength. The macroscopically occupied CDW electrons will distort the lattice when

$$1 + \kappa\chi(\mathbf{Q}, 0) = 0. \quad (7)$$

The phonon dynamic structure factor is obtained by taking the analytical continuation $i\omega_n \rightarrow \omega + i\delta$

$$S(\mathbf{q}, \omega) = \frac{-\text{Im}D(\mathbf{q}, \omega + i\delta)}{1 - e^{-\beta\omega}}. \quad (8)$$

The typical energy for the CDW metals AV_3Sb_5 and $R\text{Te}_3$ has the order of 1 eV [4, 8]. During the numerical calculations, we take the hopping amplitude t as the energy unit that has the typical value of $t = 1$ eV. The CDW-activated modes in AV_3Sb_5 and $R\text{Te}_3$ has the typical bare frequency $\Omega_0 = 0.03t$ [4, 12]. Once we set the CDW transition temperature as T_{CDW} , the interaction parameters u and κ are specified phenomenologically according to the conditions in Eqs.(5) and (7). We can tune the electron-electron and electron-phonon interactions ratio u/κ to study the evolution of the lattice dynamics. The low-temperature charge susceptibility is sensitive to the Fermi surface structure, and we firstly set $T_{\text{CDW}} = 0.001t$ and $u/\kappa = 0$ to study the phonon dynamic structure factor. The experimental typical CDW transition temperature in AV_3Sb_5 and $R\text{Te}_3$ is $T_{\text{CDW}} = 0.01t$, the same order as Ω_0 . We then set the transition temperature as $T_{\text{CDW}} = 0.01t$ and tune the ratio u/κ to discuss the relevant lattice dynamics. The DOS at Fermi surface is evaluated with the integration window $\Delta\omega = 0.01t$ in Eq.(1) and the smearing energy takes the value of $\delta = 0.001t$ for the analytical continuation $i\omega_n \rightarrow \omega + i\delta$.

Central peak and phonon hardening for kagome VHS filling. – The simple kagome band has the dispersion $\epsilon_{\mathbf{k}1,2} = (\mp\sqrt{3} + 2(\cos(k_1) + \cos(k_2) + \cos(k_1 - k_2)) - 1)t$ and $\epsilon_{\mathbf{k}3} = 2t$. Here $k_{1,2} = \mathbf{k} \cdot \mathbf{a}_{1,2}$. \mathbf{k} and $\mathbf{a}_{1,2}$ are

the wave vector and primitive unit vectors, respectively, of kagome lattice (Fig. 1(a)). Fig. 1(b) is the band dispersion along the high-symmetry direction in the Brillouin zone with the 2nd band ϵ_{k2} , marked in red, crossing the Fermi level. Fig. 1(c) is the DOS at Fermi level in which the Fermi surface is composed of corner-shared triangles with the increased VHS DOS at M points. The 2nd band dispersion ϵ_{k2} determines the low-energy properties of the kagome system and the charge density is $\rho(\mathbf{q}) = \sum_{\mathbf{k}\sigma} c_{\mathbf{k}+\mathbf{q}\sigma}^\dagger c_{\mathbf{k}\sigma}$. For the sake of simplicity, we ignore the local-site overlap matrix element $\sum_{\mathbf{k}} u_i^*(\mathbf{k}) u_i(\mathbf{k}+\mathbf{q})$ with the local electron Bloch wave package $u_i(\mathbf{k})$ [20–22]. The electron-phonon interaction matrix element is band-dependent and somehow includes the charge-density matrix element. Our results also apply to the simple square and triangular lattice at the VHS filling where the matrix element is constant.

We numerically evaluate the charge-density susceptibility $\chi_0(\mathbf{q})$ at low temperature $T = 0.00001t$ over the entire Brillouin zone as shown in Fig. 1(d). The VHS at M points favors the particle-hole scatterings connected by the CDW vectors \mathbf{Q} with $(k_1, k_2) = (0, \pi), (\pi, 0), (\pi, \pi)$, equivalent to M vectors in the Brillouin zone. Such scattering gives rise to the largest amplitude $\chi_0'(\mathbf{Q}, 0)$ with a logarithmic singularity. The branch cuts of $\chi_0(\mathbf{q})$ along Γ - M have the extremes due to the nesting of Fermi surfaces away from VHS. Fig. 1(e), (f) and (g) display the charge density susceptibility at the CDW wave vectors \mathbf{Q} at low temperatures and low frequencies. The scattering between VHS points results in a logarithmic divergence in the real part of $\chi_0'(\mathbf{Q})$ at low frequencies ($\omega < 0.01t$) and temperatures ($T < 0.01t$).

We set $T_{\text{CDW}} = 0.001t$ to see the lattice dynamics when the phonon is coupled to the VHS fluctuations at low temperature. We set $u = 0$ and fine tune κ to make sure $T_{\text{CDW}} = 0.001t$ and evaluate the phonon dynamical structure factor as shown in Fig. 1(h). The lattice dynamics is a Fano problem where the discrete phonon mode interacts with the charge-density-fluctuation continuum. The charge-density fluctuation renormalizes the phonon dynamic structural factor, resulting in an asymmetric Fano line shape at high temperatures. With decreasing temperature, the charge-density fluctuation increases at low frequency due to scattering between VHS points and develops into a low-frequency central peak in the phonon dynamic structure factor, in contrast to the Kohn Anomaly in the usual CDW metal. Furthermore, the phonon mode does not show softening as approaching T_{CDW} but hardens at low temperatures.

The above phonon properties are dubbed as the central-peak scenario and applied to the 1D spin-Peierls compound CuGeO_3 [17–19]. The phonon Green function has two poles in the central-peak regime, in contrast to a single pole in the soft phonon scenario. We analyze the pole of the retarded phonon Green function determined by the equation

$$\frac{\omega^2}{\Omega_0^2} - (1 + \kappa\chi'(q, \omega)) = 0, \quad (9)$$

by plotting lines for the functions $\frac{\omega^2}{\Omega_0^2}$ and $1 + \kappa\chi'(q, \omega)$ in Fig. 2(a). For $T_{\text{CDW}} = 0.001t$ with $|\frac{u}{\kappa}| = 0$, besides the

intentional pole at zero frequency, the phonon Green function has another pole at $\omega \sim 0.02t$, related to the bare phonon frequency $\Omega_0 = 0.03t$. The two poles lead to the central peak at zero frequency and the phonon hardening for the lattice dynamics that is coupled to the charge-density dynamics.

We set $T_{\text{CDW}} = 0.01t$ and vary the parameters u and κ to study the lattice dynamics. From Fig. 2(a), the phonon Green function has the single-pole at zero frequency for $u/\kappa = 0$. As expected, the lattice dynamics exhibit the mode softening with decreasing temperature as shown in Fig. 2(b). As we increase the ratio, the phonon Green function for $|u/\kappa| = 1$ has an extra pole at finite frequency, implying the central-peak scenario. Two poles are close to each other and different to be resolved in the dynamic structure factor as shown in Fig. 2(c). With further increasing $|u/\kappa|$, the extra pole appears at a higher frequency. The central peak at zero frequency and the high-frequency phonon hardening are resolved in Fig. 2(d) and (e).

The significant low-energy dependence of the charge-density susceptibility guarantees the two-pole structure in the phonon Green function when $1 + \kappa\chi'(\mathbf{Q}, \omega)$ increases fast

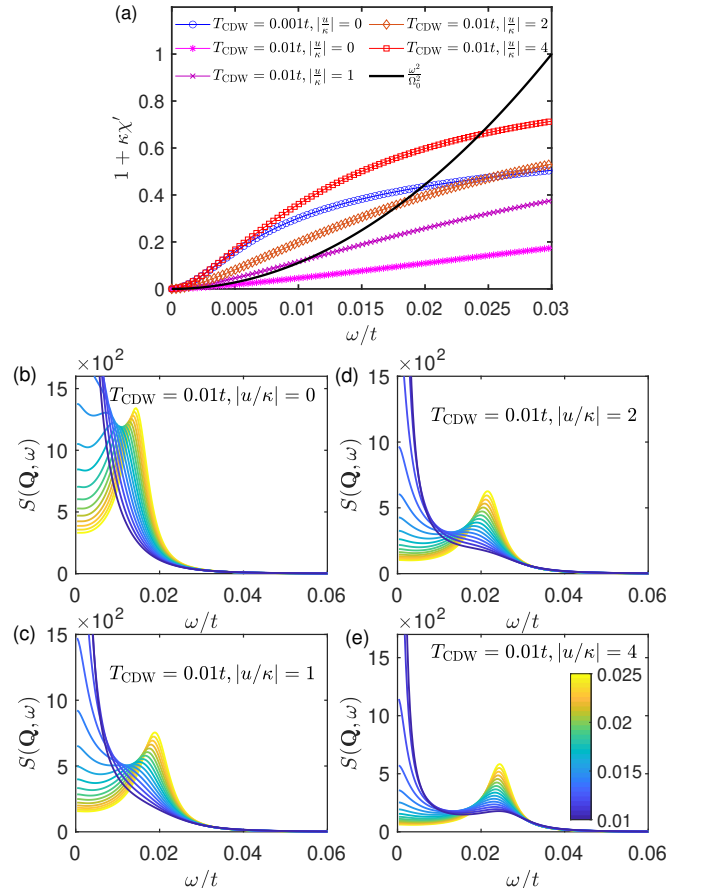


FIG. 2. Central peak for kagome VHS filling with different interaction parameters. (a) Pole analysis of the retarded phonon Green function. Temperature evolution of the dynamical structure factor $S(\mathbf{Q}, \omega)$ with $T_{\text{CDW}} = 0.01t$ with different interaction parameters with $|u/\kappa| = 0$ in (b), $|u/\kappa| = 1$ in (c), $|u/\kappa| = 2$ in (d), and $|u/\kappa| = 4$ in (e).

than the parabolic function $\frac{\omega^2}{\Omega_0^2}$. In CuGeO_3 , the associated CDW phonon frequency is ten times larger than the spin-Peierls transition temperature. Thus the two-pole structure is easily achieved. In AV_3Sb_5 , the CDW-related phonon has a comparable energy scale as the transition temperature. We need a modest effective electron-electron interaction to increase the low-energy dependence of $\chi'(\mathbf{Q}, \omega)$ for the central peak and phonon hardening. A VHS-increased low-energy charge-density susceptibility and a modest effective electron-electron interaction are essential for the central-peak regime.

Phonon softening for nearly parallel Fermi surface nesting. – Rare-earth tritellurides RTe_3 have nearly quasi-1D Fermi surface and its underlying CDW mechanism is similar to the spin-Peierls transition in CuGeO_3 . RTe_3 has the nearly parallel Fermi surface for the quasi-1D dispersion $\epsilon_{\mathbf{k}} = -2t(\cos(k_x) + \Delta \cos(k_y)) - \epsilon_F$ [4, 23], and we set $\Delta = 0.2$ and $\epsilon_F = t$. Figs. 3(a)-(f) are results corresponding to those for the kagome VHS filling in Figs. 1(c)-(h).

With $\Delta = 0$, the Fermi surface in Fig. 3(a) is the 1D system with two parallel planes where the Fermi vector is $k_F = \pm \frac{\pi}{3}$ and the nesting vector is $Q_x = 2k_F$. The finite Δ induces the k_y dispersion, and the Fermi surface has a nesting with the wave vector $\mathbf{Q} = (2k_F, \pi)$. Compared to the VHS filling results in Fig. 1, the charge-density susceptibility $\chi_0(\mathbf{q})$ in Fig. 3 distributes smoother in the Brillouin zone, consistent with multiple competing CDW wave vectors \mathbf{Q} in RTe_3 [4,

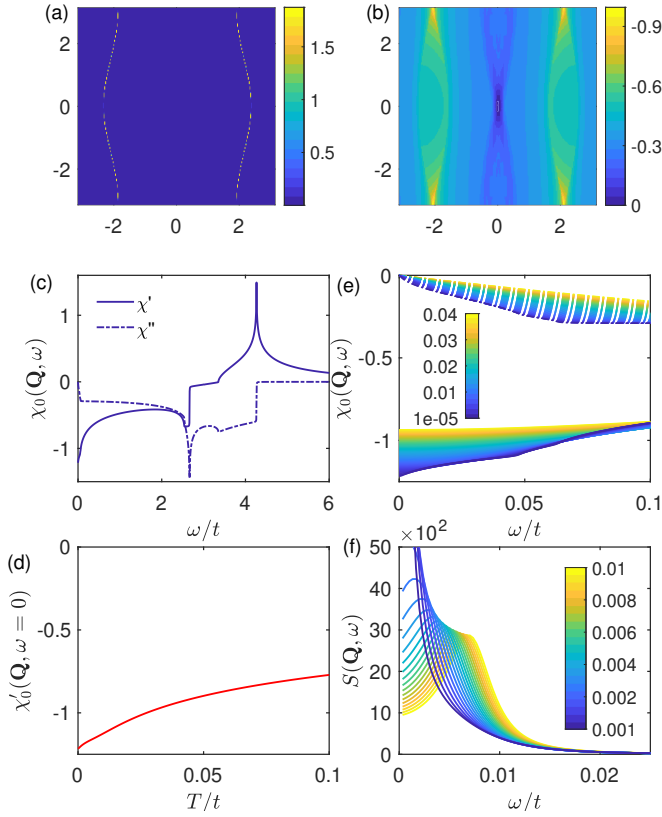


FIG. 3. Phonon softening for nearly parallel Fermi surface nesting. (a)-(f) correspond to (c)-(h) in Fig. 1.

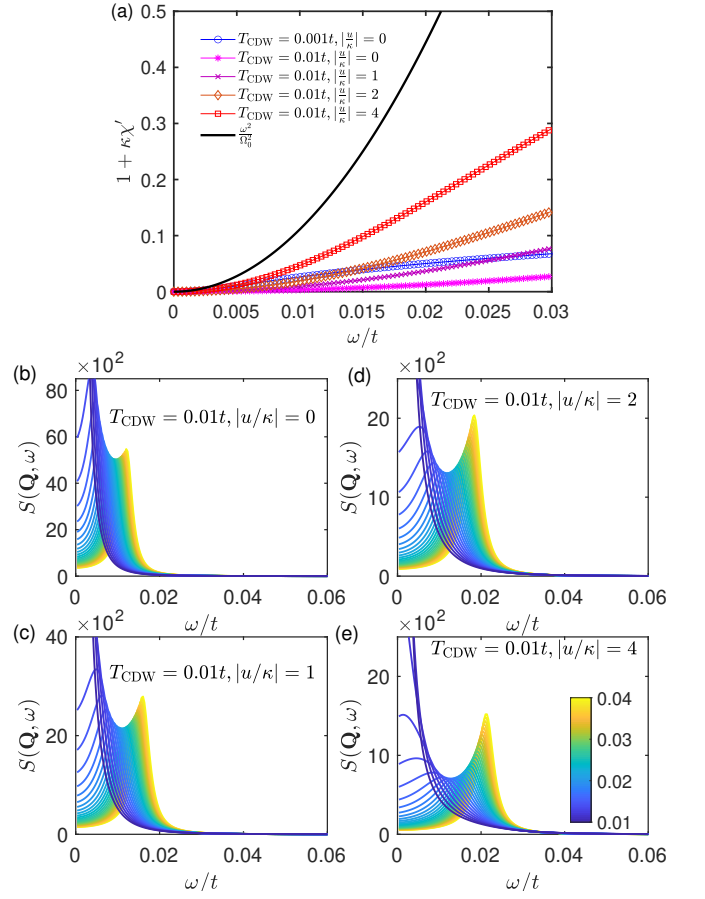


FIG. 4. Results of the CDW-activated phonon softening for nearly parallel Fermi surface nesting, similar to Fig. 2.

23]. Although there are high-energy edge singularities, the low-frequency $\chi_0(\mathbf{q}, \omega)$ is quite smooth in the frequency- and temperature-dependence. By setting $T_{\text{CDW}} = 0.001t$ with $u/\kappa = 0$, the dynamic structure factor in Fig. 3(f) displays the phonon softening and becomes divergent as decreasing the temperature to the CDW transition temperature.

The phonon softening is also resolved in the pole analysis of the retarded Green function as shown in Fig. 4(a) where the lines $\frac{\omega^2}{\Omega_0^2}$ and $1 + \kappa\chi'(\mathbf{Q}, \omega)$ has a single intersection at $\omega = 0$. We set the CDW transition temperature $T_{\text{CDW}} = 0.01t$, and different interaction parameters u and κ are selected. The corresponding $1 + \kappa\chi'(\mathbf{Q}, \omega)$ lines are also plotted in Fig. 4(a). All cases in Fig. 4(a) have no extra high energy pole beyond the zero frequency. As expected, the dynamic structure factor exhibits the phonon softening as shown in Fig. 4(b)-(f), consistent with the experimental observations in RTe_3 [4–6].

Discussions and conclusions. – In this work, we mainly study the lattice dynamics for the CDW system evolving from high temperatures to transition temperature. We present the central-peak and soft-phonon scenarios for the lattice dynamics that is coupled to different underlying electronic structures. Both scenarios have a zero-frequency peak indicating the lattice distortion formation by condensing the collective mode of the charge-density fluctuation and phonon dynamics. Below

the transition temperature, the zero-frequency mode might be split to a gapless phason mode and a gapped amplitude one. As we do not perform the self-consistent calculation below the transition temperature, such an effect is not included in the present theory.

In conclusion, we consider a simple phenomenological model to study the lattice dynamics in the charge-density-wave metal at a van-Hove-singularity filling. A VHS-enhanced low-frequency charge-density susceptibility and a modest electron-electron interaction categorize the CDW-phonon dynamics into the central-peak scenario which has a central zero-frequency peak and a hardening CDW-associated phonon mode. Our simple model may have the potential implication for the absence of the phonon softening in the kagome metal AV_3Sb_5 during the CDW transition.

ACKNOWLEDGMENTS

This work is supported by National Key Projects for Research and Development of China (Grant No. 2021YFA1400400), National Natural Science Foundation of China (NSFC) (Grant No. 11774143), the Guangdong Innovative and Entrepreneurial Research Team Program (Grants No. 2017ZT07C062), Shenzhen Key Laboratory of Advanced Quantum Functional Materials and Devices (No. ZDSYS20190902092905285), Guangdong Basic and Applied Basic Research Foundation (No. 2020B1515120100).

-
- [1] W. Kohn, Image of the fermi surface in the vibration spectrum of a metal, *Phys. Rev. Lett.* **2**, 393 (1959).
- [2] G. Grüner, The dynamics of charge-density waves, *Reviews of Modern Physics* **60**, 1129 (1988).
- [3] P. Monceau, Electronic crystals: an experimental overview, *Advances in Physics* **61**, 325 (2012), <https://doi.org/10.1080/00018732.2012.719674>.
- [4] N. Ru, *Charge Density Wave Formation in Rare-Earth Tritelurides*, Ph.D. thesis, STANFORD UNIVERSITY (2008).
- [5] M. Hoesch, A. Bosak, D. Chernyshov, H. Berger, and M. Krisch, Giant kohn anomaly and the phase transition in charge density wave $zrte_3$, *Phys. Rev. Lett.* **102**, 086402 (2009).
- [6] M. Maschek, D. A. Zocco, S. Rosenkranz, R. Heid, A. H. Said, A. Alatas, P. Walmsley, I. R. Fisher, and F. Weber, Competing soft phonon modes at the charge-density-wave transitions in $DyTe_3$, *Phys. Rev. B* **98**, 094304 (2018).
- [7] B. R. Ortiz, L. C. Gomes, J. R. Morey, M. Winiarski, M. Bordelon, J. S. Mangum, I. W. H. Oswald, J. A. Rodriguez-Rivera, J. R. Neilson, S. D. Wilson, E. Ertekin, T. M. McQueen, and E. S. Toberer, New kagome prototype materials: discovery of KV_3Sb_5 , RbV_3Sb_5 , and CsV_3Sb_5 , *Phys. Rev. Materials* **3**, 094407 (2019).
- [8] B. R. Ortiz, S. M. L. Teicher, Y. Hu, J. L. Zuo, P. M. Sarte, E. C. Schueller, A. M. M. Abeykoon, M. J. Krogstad, S. Rosenkranz, R. Osborn, R. Seshadri, L. Balents, J. He, and S. D. Wilson, CsV_3Sb_5 : A \mathbb{Z}_2 topological kagome metal with a superconducting ground state, *Phys. Rev. Lett.* **125**, 247002 (2020).
- [9] B. R. Ortiz, P. M. Sarte, E. M. Kenney, M. J. Graf, S. M. L. Teicher, R. Seshadri, and S. D. Wilson, Superconductivity in the F_2 kagome metal KV_3Sb_5 , *Phys. Rev. Materials* **5**, 034801 (2021).
- [10] B. R. Ortiz, S. M. L. Teicher, L. Kautzsch, P. M. Sarte, N. Ratcliffe, J. Harter, J. P. C. Ruff, R. Seshadri, and S. D. Wilson, Fermi surface mapping and the nature of charge density wave order in the kagome superconductor CsV_3Sb_5 (2021), [arXiv:2104.07230 \[cond-mat.str-el\]](https://arxiv.org/abs/2104.07230).
- [11] H. Li, T. T. Zhang, T. Yilmaz, Y. Y. Pai, C. E. Marvinney, A. Said, Q. W. Yin, C. S. Gong, Z. J. Tu, E. Vescovo, C. S. Nelson, R. G. Moore, S. Murakami, H. C. Lei, H. N. Lee, B. J. Lawrie, and H. Miao, Observation of unconventional charge density wave without acoustic phonon anomaly in kagome superconductors AV_3Sb_5 ($A = Rb, Cs$), *Phys. Rev. X* **11**, 031050 (2021).
- [12] Y. Xie, Y. Li, P. Bourges, A. Ivanov, Z. Ye, J.-X. Yin, M. Z. Hasan, A. Luo, Y. Yao, Z. Wang, G. Xu, and P. Dai, Electron-phonon coupling in the charge density wave state of csv_3sb_5 (2021), [arXiv:2111.00654 \[cond-mat.str-el\]](https://arxiv.org/abs/2111.00654).
- [13] X. Feng, K. Jiang, Z. Wang, and J. Hu, Chiral flux phase in the kagome superconductor AV_3Sb_5 , *Science Bulletin* **66**, 1384 (2021).
- [14] T. Park, M. Ye, and L. Balents, Electronic instabilities of kagome metals: Saddle points and landau theory, *Phys. Rev. B* **104**, 035142 (2021).
- [15] X. Wu, T. Schwemmer, T. Müller, A. Consiglio, G. Sangiovanni, D. Di Sante, Y. Iqbal, W. Hanke, A. P. Schnyder, M. M. Denner, M. H. Fischer, T. Neupert, and R. Thomale, Nature of unconventional pairing in the kagome superconductors ACs_3Sb_5 ($A = K, Rb, Cs$), *Phys. Rev. Lett.* **127**, 177001 (2021).
- [16] Y. Liu, Y. Wang, Y. Cai, Z. Hao, X.-M. Ma, L. Wang, C. Liu, J. Chen, L. Zhou, J. Wang, S. Wang, H. He, Y. Liu, S. Cui, J. Wang, B. Huang, C. Chen, and J.-W. Mei, Doping evolution of superconductivity, charge order and band topology in hole-doped topological kagome superconductors $cs(v_{1-x}ti_x)_3sb_5$ (2021), [arXiv:2110.12651 \[cond-mat.supr-con\]](https://arxiv.org/abs/2110.12651).
- [17] C. Gros and R. Werner, Dynamics of the peierls-active phonon modes in $cugeo_3$, *Phys. Rev. B* **58**, R14677 (1998).
- [18] F. Ye, G.-H. Ding, and B.-W. Xu, Dynamical properties of phonons in the XY spin chain coupled with lattices, *Phys. Rev. B* **64**, 094431 (2001).
- [19] M. Holicki, H. Fehske, and R. Werner, Magnetoelastic excitations in spin-peierls systems, *Phys. Rev. B* **63**, 174417 (2001).
- [20] W.-S. Wang, Z.-Z. Li, Y.-Y. Xiang, and Q.-H. Wang, Competing electronic orders on kagome lattices at van hove filling, *Phys. Rev. B* **87**, 115135 (2013).
- [21] S.-L. Yu and J.-X. Li, Chiral superconducting phase and chiral spin-density-wave phase in a hubbard model on the kagome lattice, *Phys. Rev. B* **85**, 144402 (2012).
- [22] M. L. Kiesel and R. Thomale, Sublattice interference in the kagome Hubbard model, *Physical Review B* **86**, 121105 (2012).
- [23] H. Yao, J. A. Robertson, E.-A. Kim, and S. A. Kivelson, Theory of stripes in quasi-two-dimensional rare-earth tellurides, *Phys. Rev. B* **74**, 245126 (2006).